

AC Loss Reduction of Superconducting Power Transmission Cables Comprising Coated Conductors

Naoyuki Amemiya, Zhenan Jiang, Masaaki Nakahata, Masashi Yagi, Shinichi Mukoyama, Naoji Kashima, Shigeo Nagaya, and Yuh Shiohara, *Non-Member, IEEE*

Abstract— AC losses in power transmission cables comprising coated conductors could be potentially small. A strategy to approach their potentially small AC loss was studied. AC losses in mono-layer conductors for cables were calculated numerically in order to show the principle for AC loss reduction: use of narrower coated conductors and/or decrease in space between conductors reduce the magnetic field component perpendicular to the wide face of coated conductors, and they are effective for AC loss reduction. This principle was confirmed experimentally by using short mono-layer conductors. Based on the principle, 1 kArms-class three-layer conductors were fabricated, and AC loss of 0.054 W/m at 1 kArms was achieved. The influence of a magnetic substrate on the AC losses in a single coated conductor and a mono-layer conductor for a cable was studied numerically.

Index Terms— AC loss, coated conductors, superconducting cables, YBCO

I. INTRODUCTION

Power transmission cable is one of the most feasible applications of high T_c superconductors [1]–[8], but AC loss reduction is critical for its commercialization. Potentially, AC losses in power transmission cables comprising coated conductors could be small because of a thin superconductor layer in coated conductors; further, cables comprising superconducting tapes have almost circular magnetic field lines. When the magnetic field is parallel to the wide face of the thin layer of a superconductor, its AC loss is small [9]. On the basis of the mono-block model where a mono-layer polygonal assembly of superconducting tapes is approximated to a thin

Manuscript received August 29, 2006. This work was supported by the New Energy and Industrial Technology Development Organization (NEDO) as Collaborative Research and Development of Fundamental Technologies for Superconductivity Applications.

N. Amemiya, Z. Jiang, and M. Nakahata are with Faculty of Engineering, Yokohama National University, Yokohama 240-8501, Japan (phone: 045-339-4119; fax: 045-338-1157; e-mail: ame@rain.dnj.ynu.ac.jp, kyo@rain.dnj.ynu.ac.jp, and naka@rain.dnj.ynu.ac.jp).

M. Yagi and S. Mukoyama are with The Furukawa Electric Co., Ltd., Ichihara 290-8555, Japan (e-mail: m-yagi@ch.furukawa.co.jp and mukoyama@ch.furukawa.co.jp).

N. Kashima and S. Nagaya are with Chubu Electric Power Co., Inc., Nagoya 459-8522, Japan (e-mail: Kashima.Naoji@chuden.co.jp and Nagaya.Shigeo@chuden.co.jp).

Y. Shiohara is with the Superconductivity Research Laboratory, ISTE, Tokyo 135-0062, Japan (e-mail: shiohara@istec.or.jp).

superconducting cylinder whose thickness is the same as the thickness of the superconductor layer of the tapes [10], the AC loss energy of the cable per unit length per cycle is

$$Q_{MB} = \frac{I_c^2 \mu_0}{2\pi h^2} \left\{ \left(2 - \frac{I_t}{I_c} h \right) \frac{I_t}{I_c} h + 2 \left(1 - \frac{I_t}{I_c} h \right) \ln \left(1 - \frac{I_t}{I_c} h \right) \right\}, \quad (1)$$

where I_c is the critical current, I_t is the peak value of the transport current, and h is defined as

$$h = \frac{D_1^2 - D_2^2}{D_1^2}, \quad (2)$$

Here, D_1 and D_2 are the outer and inner diameters of the superconducting cylinder, respectively. The AC loss power per unit length, P_{MB} , is defined as $Q_{MB}f$, where f is the frequency of the current. For example, when $D_1 = 20$ mm, $D_2 = 20$ mm – 0.002 mm, the critical current density $J_c = 3 \times 10^{10}$ A/m² ($I_c = \pi\{(D_1/2)^2 - (D_2/2)^2\}J_c = 1885$ A), and $I_t/I_c = 0.7$ ($I_t = 1319$ A), $P_{MB} = 8.126 \times 10^{-4}$ W/m. The actual AC loss is much larger than this ideal value of P_{MB} because of many non-ideal factors.

The objectives of this study are showing a strategy to approach potentially small AC loss in power transmission cables comprising coated conductors and demonstrating the AC loss reduction experimentally. We assume that a uniform current distribution between layers is attained in multi-layer cables by pitch adjustment. First, we point out the importance of reducing the magnetic field component perpendicular to the wide face of the coated conductors in order to reduce the AC loss; AC losses in mono-layer conductors for cables with various cross-sectional configurations are calculated numerically in order to show the principle of AC loss reduction. This principle is confirmed experimentally by using a couple of short mono-layer conductors. Based on this principle, 1 kArms-class multi-layer conductors are designed and fabricated to demonstrate the AC loss reduction. Finally, the influence of a magnetic substrate on the AC losses in cables is studied numerically.

4LW03

2

II. REDUCTION IN PERPENDICULAR MAGNETIC FIELD COMPONENT AND AC LOSSES

The AC loss due to the magnetic field component parallel to the wide face of coated conductors (parallel magnetic field component) is so small that the AC loss generated by a small but finite magnetic field component perpendicular to the wide face of coated conductors (perpendicular magnetic field component) should dominate the AC loss in coated conductors which compose a conductor for the cable. Therefore, the reduction in the perpendicular magnetic field component is a key for the AC loss reduction. In this section, we focus on mono-layer conductors for a cable to show a method to reduce the perpendicular magnetic field component for reducing AC losses.

A. Numerical Calculation of AC Losses in Mono-Layer Conductors

The electromagnetic field of a coated conductor in mono-layer conductors was numerically analyzed to calculate its AC loss. The analysis was performed in a cross section of a coated conductor by the finite element method. In the analysis, both the perpendicular and parallel magnetic field components were taken into consideration. The superconducting property is given by the power law electric field – current density (E - J) characteristic

$$E = E_0 \left(\frac{J}{J_c} \right)^n, \quad (3)$$

where J_c is the critical current density and $E_0 = 1 \times 10^{-4}$ V/m [11]. The AC losses can be calculated from the temporal evolution of the current density and electric field. In the numerical analysis, we varied a cross section of a mono-layer conductor with a polygonal rather than a perfectly circular shape; the conductor is an assembly of flat coated conductors with finite space between coated conductors, as shown in Fig. 1. We varied the number of coated conductors in a mono-layer conductor and the space between coated conductors, which could influence the magnitude of the perpendicular magnetic field component. The specifications of the mono-layer conductors are listed in Table I. In the table, 1C-A is a standard mono-layer conductor comprising fifteen 4 mm wide coated conductors and others are its variations. The amplitude of the transport current of an entire mono-layer conductor, I_t , was kept at 1440 A, and its frequency f was 50 Hz. The magnetic flux lines near the edge of a coated conductor are shown for 1C-A, 1C-B, and 1C-C in Figs. 2(a), (b), and (c), respectively. In each figure, the dash-dot-dash line represents the center of the space between conductors. As compared to 1C-A, the magnetic flux lines are more parallel to the wide face of the conductor in 1C-B comprising a larger number of narrower conductors with a smaller space between the conductors. A larger magnetic flux than that in 1C-A penetrates the larger space between the conductors in 1C-C. Consequently, at the edge of the conductor, the perpendicular magnetic field component is larger in 1C-C and smaller in 1C-B when compared to 1C-A. The lateral

distributions of the loss power density in a conductor are shown in Fig. 3. In Figs. 2 and 3, a larger perpendicular magnetic field component leads to larger loss power density near the edges of a conductor; a large loss at the edge of a conductor dominates the AC loss of the entire conductor. In Fig. 4, the calculated AC loss in each mono-layer conductor normalized with I_c^2 , where I_c is the critical current of the entire mono-layer conductor,

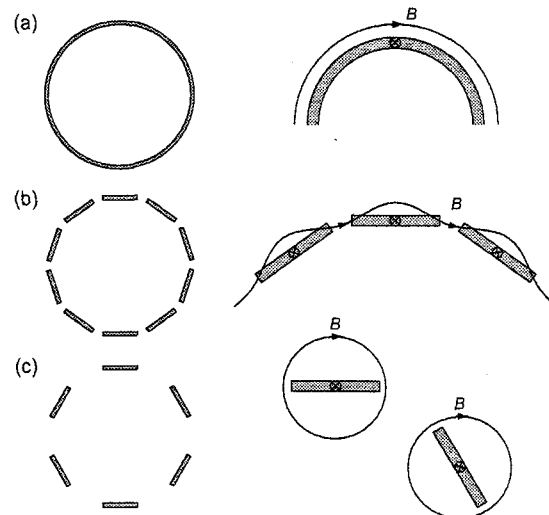


Fig. 1. Schematic cross sections of conductors for cables: (a) mono-block model, (b) a polygonal assembly of conductors, and (c) a polygonal assembly of conductors with large space between conductors.

TABLE I
SPECIFICATIONS OF MONO-LAYER CONDUCTORS FOR ANALYSIS

Conductor name	1C-A	1C-B	1C-C
^a Diameter	19.8 mm	20 mm	20.7 mm
Number of conductors	15	30	15
Conductor width	4 mm	2 mm	4 mm
Superconductor layer thickness	2 μ m	2 μ m	2 μ m
Space between conductors	0.2 mm	0.1 mm	0.4 mm
Total critical current	1800 A	1800 A	1800 A
n value	20	20	20

^a Diameter of inscribed circle of assembly of coated conductors. These values are used as D_2 in (2).

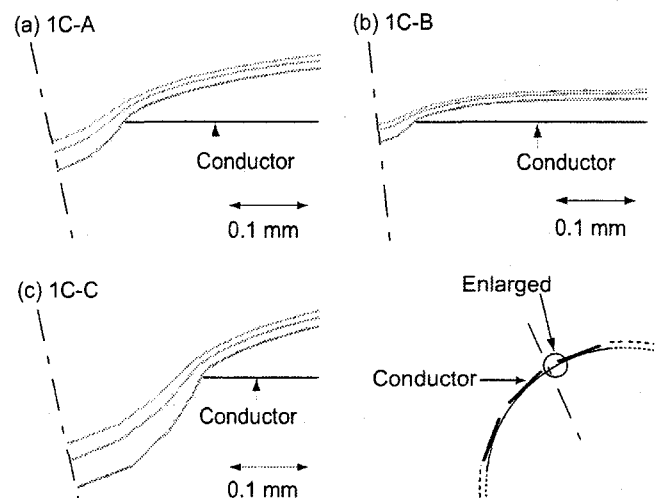


Fig. 2. Magnetic flux lines near edge of coated conductors in 1C-A, 1C-B, and 1C-C.

4LW03

3

Q_{MB}/I_c^2 , and the normalized loss by Norris Q_{NS}/I_c^2 are plotted against I_t/I_c . Here, Q_{NS} is defined as

$$Q_{NS} = N \frac{I_{cc}^2 \mu_0}{\pi} \left\{ \left(1 - \frac{I_t}{I_c} \right) \ln \left(1 - \frac{I_t}{I_c} \right) + \left(1 + \frac{I_t}{I_c} \right) \ln \left(1 + \frac{I_t}{I_c} \right) - \left(\frac{I_t}{I_c} \right)^2 \right\}, \quad (4)$$

where N is the number of conductors in the mono-layer conductor and $I_{cc} = I_c/N$ [12]. P_{NS} is defined as $Q_{NS}f$. The AC loss in 1C-B with a smaller perpendicular magnetic field is smaller than that in 1C-A, and the AC loss in 1C-C with a larger perpendicular magnetic field component is larger than that in 1C-A.

These numerical results show that a smaller conductor width and a smaller space between conductors are effective to reduce AC losses.

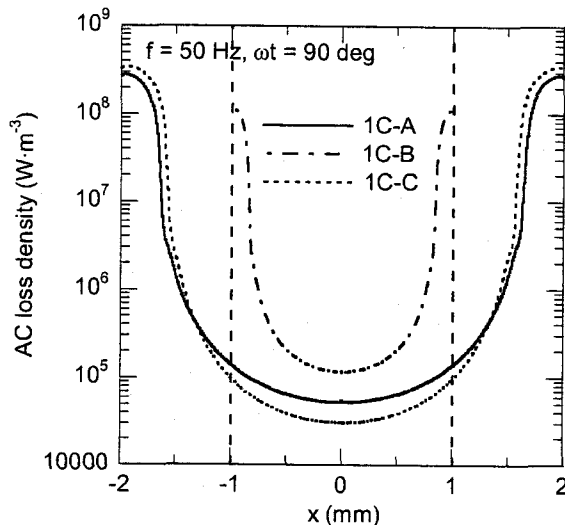


Fig. 3. Lateral distributions of loss power density in 1C-A, 1C-B, and 1C-C.

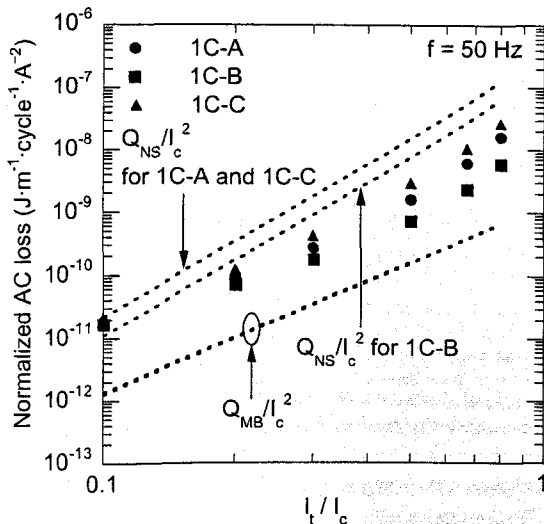


Fig. 4. Calculated AC losses in 1C-A, 1C-B, and 1C-C normalized with I_c^2 , Q_{MB}/I_c^2 , and Q_{NS}/I_c^2 .

B. AC Loss Measurements of Mono-Layer Conductors with Different Conductor Widths and Different Spaces between Conductors

Six 10 mm wide and 300 mm long coated conductors fabricated by the IBAD/MOCVD method were prepared to make short mono-layer conductors whose specifications are listed in Table II. The listed critical current of each mono-layer conductor is the sum of the measured critical current of coated conductors composing each mono-layer conductor.

First, six coated conductors were assembled on a GFRP former whose diameter is 20 mm (1C-ND). All the coated conductors were straight, not spiral, and parallel to the axis of a mono-layer conductor. Usually, all the conductors in a cable are connected in parallel and carry AC transport current. However, the mono-layer conductors used in the experiments are so short that a slight difference in the resistance between each coated conductor and current lead easily results in a non-uniform current distribution. Therefore, the six coated conductors were connected in series rather than parallel, and AC current was supplied using a bipolar power supply and transformer. This series connection ensures uniform current distribution between conductors, while the electromagnetic field distributions in both the connections are identical; hence, the generated AC losses should be identical. Two voltage taps were attached to one coated conductor to measure the AC loss; a lead loop for the voltage taps was wound spirally around the entire mono-layer conductor. The AC loss energy of an entire mono-layer conductor per unit length per cycle is obtained as

$$Q_t = \frac{1}{d} \frac{I_{t,rms} V_{t,in,rms}}{f}, \quad (5)$$

where d is the distance between the voltage taps, which is 100 mm in the samples; $I_{t,rms}$, the root-mean-square of the transport current of the entire mono-layer conductor, which is the product of the current in one coated conductor and the number of coated conductors; $V_{t,in,rms}$, the root-mean-square of the loss component of the tap voltage obtained using a lock-in amplifier. f is 65.44 Hz in the experiments.

Next, 1C-ND was disassembled. Each coated conductor was divided into three 3.18 mm wide conductors using a laser, and the divided conductors were assembled on a GFRP former whose diameter was 19.2 mm (1C-D3S). The AC loss of 1C-D3S was measured in the same manner as 1C-ND.

Finally, the former of 1C-D3S was replaced with a 20 mm former (1C-D3L). The AC loss of this mono-layer conductor

TABLE II
SPECIFICATIONS OF MONO-LAYER CONDUCTORS FOR EXPERIMENTS

Conductor name	1C-ND	1C-D3S	1C-D3L
Former diameter	20 mm	19.2 mm	20 mm
Number of conductors	6	18	18
Conductor ^a width	10 mm	3.18 mm	3.18 mm
YBCO layer thickness	1 μm	1 μm	1 μm
Average space between conductors	0.47 mm	0.17 mm	0.31 mm
Total critical current	885.7 A	861.1 A	819.5 A

^a Coated conductors were laminated with 0.1 mm thick copper tape.

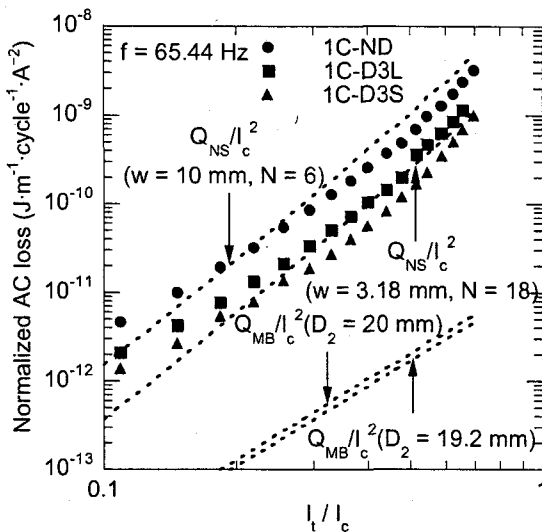


Fig. 5. Measured AC losses in 1C-ND, 1C-D3L, and 1C-D3S, Q_{NS}/I_c^2 , and Q_{MB}/I_c^2 .

was also measured.

In Fig. 5, the measured losses in each mono-layer conductor normalized with I_c^2 , Q_{MB}/I_c^2 , and Q_{NS}/I_c^2 are plotted against I_t / I_c . The measured loss is smallest in 1C-D3S comprising divided conductors with a smaller space between conductors and is largest in 1C-ND comprising undivided wide conductors. These experimental results are qualitatively consistent with the numerical results shown in Fig. 4. It should be noted that the measured loss of 1C-ND is smaller than Q_{NS} ($w = 10$ mm and $N = 6$), and that of 1C-D3S is smaller than Q_{NS} ($w = 3.18$ mm and $N = 18$). In a mono-layer conductor where the coated conductors are assembled in a polygonal shape, the self magnetic fields of adjacent coated conductors cancel each other, and the magnetic field component perpendicular to the wide face of the conductor decreases. Hence, the measured losses are smaller than Q_{NS} .

III. DEMONSTRATION OF AC LOSS REDUCTION IN MULTI-LAYER CONDUCTORS

Here, we assume a uniform current distribution between layers. This is attained in practical conductors for a cable by adjusting the spiral pitch of each layer.

Based on the principle for the AC loss reduction obtained in II, two 1 kArms-class three-layer conductors whose specifications are listed in Table III were designed and fabricated using IBAD/MOCVD coated conductors. The listed critical current of each layer or entire three-layer conductor is the sum of the measured critical current of the coated conductors composing each layer or entire three-layer conductor. 3C-A is a three-layer conductor comprising eighty-five 1.8 mm wide conductors, and 3C-B is a three-layer conductor comprising fifty-one 3.1 mm wide conductors. In both three-layer conductors, the length of the coated conductors in the outermost layer is 240 mm, and that of the coated conductors in the innermost layer is 400 mm, respectively. All the coated conductors are straight, not spiral, and parallel to the

axis of a three-layer conductor. To ensure a uniform current distribution between the layers and to perform the experiments using a power supply with limited output current, three layers were connected in series, and AC current was supplied using a bipolar power supply and transformer. This series connection of the three layers does not affect the electromagnetic field distribution and generated AC losses. Two rings of copper wires were soldered to all the conductors in the outermost layer. These two rings are used as the voltage taps; a lead loop for the voltage taps was wound spirally around the entire three-layer conductor. The distance between two voltage taps d is 100 mm. The AC loss energy of an entire three-layer conductor per unit length per cycle can be obtained using (5), where $I_{t,rms}$ is the transport current (rms) of the entire three-layer conductor, which is the current in one layer multiplied by three.

In Fig. 6, the measured loss in each three-layer conductor and P_{NS} are plotted against $I_{t,rms}$. Since the experiments were performed at $f = 65.44$ Hz and 50 Hz, the AC loss values were converted to the values at 50 Hz so that they could be plotted in one figure. The AC loss of 0.054 W/m at 1 kArms attained in 3C-A is the lowest ever reported AC loss in conductors for superconducting power transmission cables. In Table IV, the measured AC losses of 3C-A, 3C-B, and a couple of cables made with BSCCO multifilamentary tapes are compared with each other at $I_{t,rms} = 1$ kArms [1], [13]. The AC loss in BSCCO cable BiC-1 is 0.09 W/m, but it should be noted that its diameter is considerably larger than the diameter of 3C-A or that of 3C-B. BiC-2 has almost the same diameter as 3C-A and 3C-B, but its AC loss is considerably larger than the AC losses of 3C-A and 3C-B. In Fig. 6, the measured losses in three-layer conductors are larger than P_{NS} , whereas the measured losses in mono-layer conductors are smaller than Q_{NS} as shown in Fig. 5. In multi-layer conductors, the coated conductors in the outer layer are exposed to the magnetic field generated by the current in inner layers. This magnetic field increases the AC loss in

TABLE III
SPECIFICATIONS OF THREE-LAYER CONDUCTORS FOR EXPERIMENTS

Conductor name	3C-A	3C-B
Outer diameter	19.6 mm	19.6 mm
Inner diameter of layer 1	17.3 mm	17.0 mm
Inner diameter of layer 2	17.9 mm	18.1 mm
Inner diameter of layer 3	19.2 mm	19.2 mm
Conductor number of layer 1	27	16
Conductor number of layer 2	28	17
Conductor number of layer 3	30	18
Conductor ^a width	1.8 mm	3.1 mm
YBCO layer thickness	1.4 μ m	1.4 μ m
Average space between conductors in layer 1	0.21 mm	0.24 mm
Average space between conductors in layer 2	0.20 mm	0.24 mm
Average space between conductors in layer 3	0.21 mm	0.25 mm
Critical current of layer 1	699 A	734 A
Critical current of layer 2	705 A	771 A
Critical current of layer 3	778 A	796 A
Total critical current	2183 A	2301 A

^a Coated conductors were laminated with 0.1 mm thick copper tape.

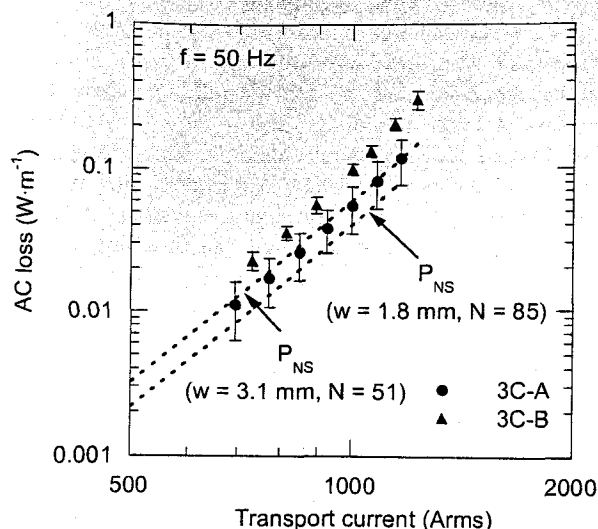


Fig. 6. Measured AC losses in 3C-A and 3C-B, and P_{NS} .

TABLE IV
COMPARISON OF AC LOSSES IN VARIOUS CONDUCTORS/CABLES

Conductor/cable name	3C-A	3C-B	BiC-1 ^a	BiC-2 ^b
Outer diameter	19.6 mm	19.6 mm	37.9 mm	20 mm
Critical current	2183 A	2301 A	5310 A	2770 A
AC loss at 1 kArms	0.054 W/m	0.097 W/m	0.09 W/m	0.4 W/m ^c

* AC loss is the value for core excluding shield for one phase.

^a BiC-1: Super-Ace short cable [13].

^b BiC-2: TEPCO/SEI 100 m cable [1].

^c The AC loss value in [1] is 0.7 W/m/phase at 1 kArms. The AC loss in the core is estimated as 0.4 W/m using the UCD model.

conductors in the outer layer [14]. Hence, the measured losses in three-layer cables are larger than P_{NS} .

IV. INFLUENCE OF MAGNETIC SUBSTRATE ON AC LOSS IN CONDUCTOR FOR CABLE

Cost reduction of coated conductors is another key issue for the commercialization of superconducting power transmission cables. Biaxially-textured metal substrates are often preferred to IBA substrates from the viewpoint of cost reduction. However, biaxially-textured metal substrates are usually Ni-alloy and magnetic. Their magnetic properties can influence AC losses in coated conductors and cables.

Numerical electromagnetic field analysis was performed for single coated conductors with and without a magnetic substrate and for mono-layer conductors comprising coated conductors with and without a magnetic substrate. In principle, the numerical model is same as that in II.A. The specifications of the single coated conductors are listed in Table V, while those of the mono-layer conductors are listed in Table VI. The superconductor layer thickness is assumed to be 10 μm to reduce the cross-sectional aspect ratio so that the efficiency of numerical calculations is improved.

In Figs. 7(a), (b), (c), and (d), magnetic flux lines are shown for $T (\mu_s = 1)$, $T (\mu_s = 1000)$, $1C (\mu_s = 1)$, and $1C (\mu_s = 1000)$, respectively. In the case of single coated conductors (Figs. 7(a)

and 7(b)), a magnetic substrate attracts the magnetic flux produced by the transport current, and the magnetic flux distribution is drastically changed by the magnetic substrate—the perpendicular magnetic field component increases. In Fig. 8, the lateral distribution of the loss power density in $T (\mu_s = 1)$ and that in $T (\mu_s = 1000)$ are shown. In $T (\mu_s = 1000)$, a larger perpendicular magnetic field component leads to a larger loss generation near the edge of the conductor

TABLE V
SPECIFICATIONS OF SINGLE COATED CONDUCTORS WITH/WITHOUT MAGNETIC SUBSTRATE FOR ANALYSIS

Conductor name	$T (\mu_s = 1)$	$T (\mu_s = 1000)$
Conductor width	5 mm	5 mm
Superconductor layer thickness	10 μm	10 μm
Relative magnetic permeability, μ_s	1	1000
Critical current	100 A	100 A
n value	30	30

TABLE VI
SPECIFICATIONS OF MONO-LAYER CONDUCTORS WITH/WITHOUT MAGNETIC SUBSTRATE FOR ANALYSIS

Conductor name	$1C (\mu_s = 1)$	$1C (\mu_s = 1000)$
Former diameter	19.2 mm	19.2 mm
Number of conductors	12	12
Conductor width	5 mm	5 mm
Superconductor layer thickness	10 μm	10 μm
Substrate thickness	0.1 mm	0.1 mm
Space between conductors	0.2 mm	0.2 mm
Relative magnetic permeability, μ_s	1	1000
Total critical current	1200 A	1200 A
n value	30	30

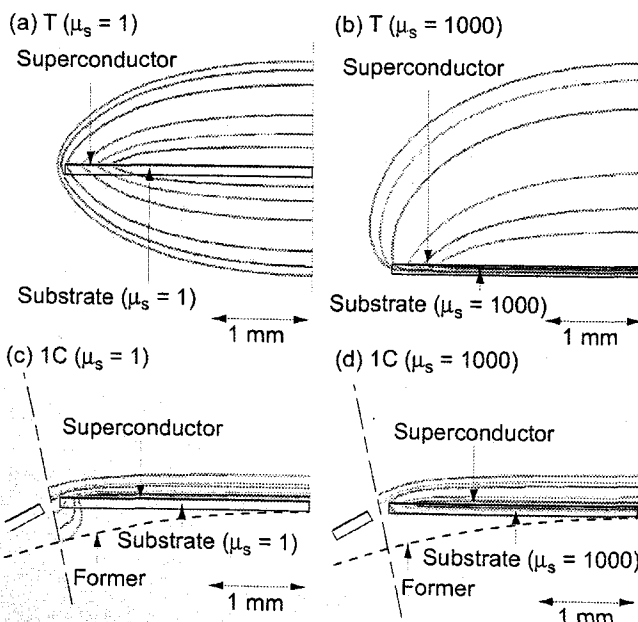


Fig. 7. Magnetic flux lines near edge of coated conductors in $T (\mu_s = 1)$, $T (\mu_s = 1000)$, $1C (\mu_s = 1)$, and $1C (\mu_s = 1000)$.

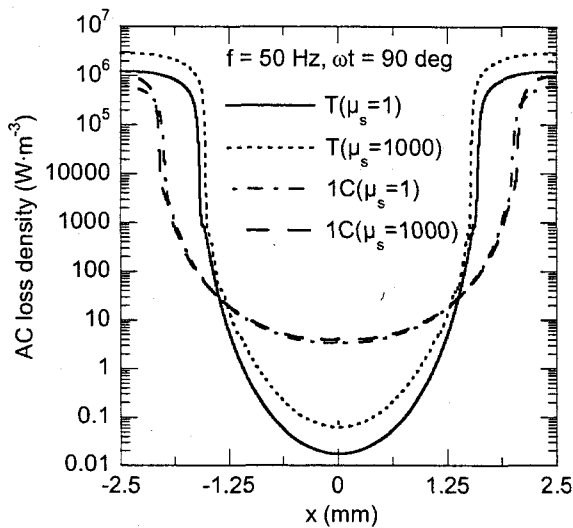


Fig. 8. Lateral distributions of loss power density in coated conductors in $T(\mu_s = 1)$, $T(\mu_s = 1000)$, $1C(\mu_s = 1)$, and $1C(\mu_s = 1000)$.

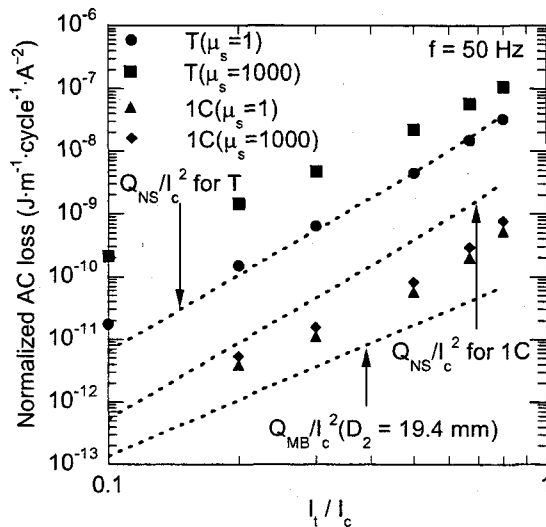


Fig. 9. Calculated AC losses in $T(\mu_s = 1)$, $T(\mu_s = 1000)$, $1C(\mu_s = 1)$, and $1C(\mu_s = 1000)$ normalized with I_c^2 , Q_{MB}/I_c^2 , and Q_{NS}/I_c^2 .

as compared to $T(\mu_s = 1)$. In mono-layer conductors (Figs. 7(c) and 7(d)), most of the magnetic flux lines lie outside the layer of the coated conductors, and the magnetic substrate inside the layer of the coated conductor does not change the magnetic flux distribution drastically. In Fig. 8, the lateral distributions of the loss power density in $1C(\mu_s = 1)$ and $1C(\mu_s = 1000)$ are almost identical. In Fig. 9, the calculated AC loss in each single coated conductor normalized with I_c^2 , that in each mono-layer conductor normalized with I_c^2 , Q_{MB}/I_c^2 , and Q_{NS}/I_c^2 are plotted against I_t / I_c . In mono-layer conductors, the influence of the magnetic substrate on the AC loss is small, whereas a magnetic substrate remarkably increases the AC loss in the single coated conductor.

V. CONCLUSION

AC losses in power transmission cables comprising coated

conductors are determined by the magnetic field component perpendicular to the wide face of coated conductors. The use of a large number of narrow conductors and a decrease in the space between conductors are effective to reduce AC losses. The AC loss of 0.054 W/m at 1 kArms was achieved in a three-layer conductor whose outer diameter is 19.6 mm. An increase in AC losses by a magnetic substrate is not as remarkable in a mono-layer conductor as in a single coated conductor.

REFERENCES

- [1] S. Honjo, M. Shimodate, Y. Takahashi, T. Masuda, H. Yumura, C. Suzawa, S. Isojima, and H. Suzuki, "Electric properties of a 66 kV 3-core superconducting power cable system," *IEEE Trans. Appl. Supercond.*, vol. 13, pp. 1952–1955, Jun. 2003.
- [2] S. Mukoyama, S. Maruyama, M. Yagi, N. Ishii, H. Kimura, H. Suzuki, M. Ichikawa, T. Takahashi, T. Okamoto, A. Kimura, and K. Yasuda, "Demonstration and verification tests of a 500 m HTS cable in the super-ACE project," *Physica C*, vol. 426–431, pp. 1365–1373, 2005.
- [3] J. F. Maguire, F. Schmidt, F. Hamber, and T. E. Welsh, "Development and demonstration of a long length HTS cable to operate in the long island power authority transmission grid," *IEEE Trans. Appl. Supercond.*, vol. 15, pp. 1787–1792, Jun. 2005.
- [4] C. S. Weber, C. T. Reis, A. Dada, T. Masuda, and J. Moscovici, "Overview of the underground 34.5 kV HTS power cable program in Albany, NY," *IEEE Trans. Appl. Supercond.*, vol. 15, pp. 1793–1797, Jun. 2005.
- [5] Y. Xin, B. Hou, Y. Bi, H. Xi, Y. Zhang, A. Ren, X. Yang, Z. Ham, S. Wu, and H. Ding, "Introduction of China's first live grid installed HTS power cable system," *IEEE Trans. Appl. Supercond.*, vol. 15, pp. 1814–1817, Jun. 2005.
- [6] M. J. Gouge, D. T. Lindsay, J. A. Demko, R. C. Duckworth, A. R. Ellis, P. W. Fisher, D. R. James, J. W. Lue, M. L. Roden, I. Sauers, J. C. Tolbert, C. Traeholt, and D. Willen, "Tests of tri-axial HTS cables," *IEEE Trans. Appl. Supercond.*, vol. 15, pp. 1827–1830, Jun. 2005.
- [7] J. Cho, K.-D. Sim, J.-H. Bae, H.-J. Kim, J.-H. Kim, K.-C. Seong, H.-M. Jang, C.-Y. Lee, and D.-Y. Koh, "Design and experimental results of a 3 phase 30 m HTS power cable," *IEEE Trans. Appl. Supercond.*, vol. 16, pp. 1602–1605, Jun. 2006.
- [8] S. Mukoyama, M. Yagi, H. Hirano, Y. Yamada, T. Izumi, and Y. Shiohara, "Development of HTS power cable using YBCO coated conductor," *Physica C*, to be published.
- [9] M. N. Wilson, *Superconducting Magnets*. Oxford: Oxford University Press, 1983, pp. 162–174.
- [10] G. Velleo and P. Metra, "An analysis of the transport losses measured on HTSC single-phase conductor prototypes," *Supercond. Sci. Technol.*, vol. 8, pp. 476–483, 1995.
- [11] N. Amemiya, S. Murasawa, N. Banno, and K. Miyamoto, "Numerical modelings of superconducting wires for AC loss calculations," *Physica C*, vol. 310, pp. 16–29, 1998.
- [12] W. T. Norris, "Calculation of hysteresis losses in hard superconductors carrying AC: Isolated conductors and edges of thin sheets," *J. Phys. D: Appl. Phys.*, vol. 3, pp. 489–507, 1970.
- [13] M. Yagi, S. Tanaka, S. Mukoyama, M. Mimura, H. Kimura, S. Torii, S. Akita, and A. Kikuchi, "Measurement of AC losses in an HTS conductor by calorimetric method," *Phys. C*, vol. 392–396, pp. 1124–1128, 2003.
- [14] S. Sato and N. Amemiya, "Electromagnetic field analysis of YBCO coated conductors in multi-layer HTS cables," *IEEE Trans. Appl. Supercond.*, vol. 16, pp. 127–130, Jun. 2006.